

Solution NMR Evidence for Symmetry in Functionally or Crystallographically Asymmetric Homodimers

Raquel Godoy-Ruiz,[†] Anna Krejcirikova,[†] D. Travis Gallagher,[‡] and Vitali Tugarinov^{*,†}

[†]Department of Chemistry and Biochemistry, University of Maryland, College Park, Maryland, 20742, United States

[‡]Biochemical Science Division, National Institute of Standards and Technology, Gaithersburg, Maryland, 20899, United States

S Supporting Information

ABSTRACT: A recurrent theme of many structural studies of homo-oligomeric protein systems is concerned with verification that the conformation observed in a crystal represents the functionally relevant structure. An asymmetric conformation adopted by two chemically identical subunits in homo-oligomers can represent an intrinsic property of a protein or be an artifact induced by crystal packing forces. Solution NMR studies can distinguish between these two possibilities. Using methyl-based NMR spectroscopy, we provide evidence for symmetry in the absence of ligands in several homodimeric proteins that are either asymmetric functionally and/or adopt different conformations of the two subunits in available X-ray structures.

An asymmetric conformation adopted by two chemically identical subunits in a homodimeric protein can represent its intrinsic structural property or be artifactual because of crystal packing forces.^{1–3} X-ray crystallography frequently provides us with a symmetric model of a homodimer when functionally the protein is known to behave asymmetrically. Conversely, crystallographic asymmetry may be present that does not exist in solution. The structurally relevant character of crystallographically observed asymmetry may be justified when it is associated with asymmetry at the subunit interface, when it is persistent under several different crystal environments, and/or when a chemical basis for the asymmetry can be identified.^{1,2} In many cases, however, slight conformational differences arise from individual subunits of a homo-oligomer being “trapped” in different crystal lattice environments.² On the other hand, when a homodimer is predicted to be asymmetric in solution on the basis of biochemical and functional assays (e.g., its subunits displaying cooperativity in ligand/substrate binding), an issue arises whether such asymmetry is “pre-existent” or induced by external stimuli such as, for example, the binding of ligands.

Since NMR chemical shifts are exquisitely sensitive to minute changes in conformation, solution NMR can distinguish between the true and spurious structural asymmetry. Until recently, many of the homo-oligomeric protein systems have been beyond the reach of solution NMR techniques because of molecular size limitations. Isotope labeling and NMR methods developed for high-molecular-weight proteins in the past decade are now well poised to address this problem.^{4–6} Here, we provide NMR evidence for symmetry in a number of ligand-free homodimeric proteins that are either asymmetric functionally (and are predicted to possess pre-existent asymmetry of its subunits in

solution) or adopt different conformations of the two identical subunits in available X-ray structures.

Recently, we have initiated NMR studies of tyrosyl tRNA synthetase^{7,8} from the thermophilic organism *Bacillus stearothermophilus* (*Bst*-YRS) as a prototype system for understanding the relationship between structural and functional asymmetry in homodimeric proteins. YRS is a paradigmatic example of a “half-site-reactive” homodimer (MW = 95 kDa).^{7,9,10} It catalyzes the activation of Tyr via formation of Tyr-AMP and subsequent transfer of the activated Tyr to the cognate tRNA^{Tyr}. The truncated form of the enzyme lacking the C-terminal tRNA-binding domain (Δ YRS; MW = 72 kDa) can activate Tyr with the same efficiency as the full-length YRS but cannot charge tRNA.¹¹ Crystal structures of *Bst*-YRS have been solved: free, in complexes with Tyr-AMP and inhibitors.¹² The structure of the C-terminal domain of YRS (not observed in any of the available X-ray structures) has been solved separately by solution NMR.¹³ All X-ray structures including that of ligand-free YRS feature a homodimer with 2-fold symmetry.^{12,14}

YRS exhibits “half-of-the-sites” activity (extreme form of negative cooperativity) with respect to Tyr binding, Tyr-AMP formation, and tRNA charging; it binds to, activates, and charges tRNA with only 1 mol of Tyr per mole of dimer.^{15,16} Earlier, it was predicted to be asymmetrical in solution in the absence of ligands from extensive kinetic and mutagenesis studies of Fersht and co-workers.^{7,16} Specifically, heterodimers between the full-length YRS and its truncated form (Δ YRS) were constructed. Such heterodimers have two sites for formation of Tyr-AMP intermediate but only one site for tRNA binding.¹¹ A mutation that drastically reduces the rate of Tyr-AMP formation has been introduced into the binding site of a predetermined subunit. It was found that heterodimers containing mutation on either subunit form 1/2 mol of Tyr-AMP/mole of dimer rapidly at the wild-type rate, while the remaining 1/2 mol are formed 10⁴-fold slower, at the rate consistent with the mutant. It was concluded from these and other experiments that the dimer is “frozen” in two states: one-half is active on one subunit and one-half on the other.^{7,16} The YRS dimer has been for many years the most compelling case of pre-existent asymmetry in a homodimeric protein despite an utter contradiction with available symmetric crystal structures.^{12,14} Although very slight differences between the conformations of the two subunits have been observed in the X-ray structure of Tyr-bound Δ YRS, it cannot apparently be related to “half-site” activity, as both subunits in the crystal structure have Tyr molecules bound.¹⁴

Received: July 29, 2011

Published: November 10, 2011

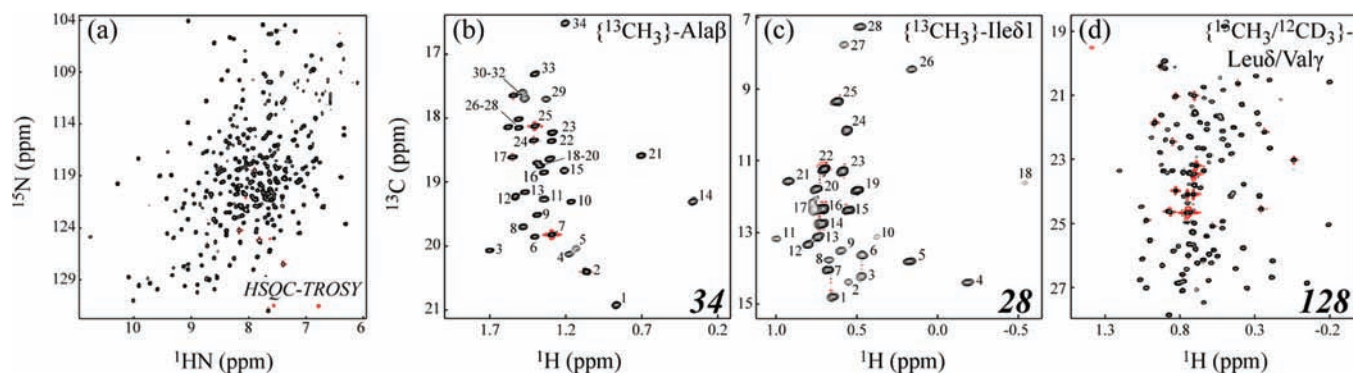


Figure 1. (a) ^1H – ^{15}N HSQC-TROSY correlation map of full-length [^2H , ^{15}N]-*Bst*-YRS (800 MHz, 50 °C). (b–d) ^1H – ^{13}C methyl-TROSY maps showing [$^{13}\text{CH}_3$]-methyl correlations of (b) Ala^β , (c) $\text{Ile}^{\delta 1}$, and (d) $\text{Leu}^\delta/\text{Val}^\gamma$. The number of residues of each type in the amino-acid sequence of *Bst*-YRS is shown in bold italics at the right bottom corners of panels (b–d). The number of identifiable separated cross-peaks in (d) is 124 at 800 MHz. The spectra in (b–d) have been acquired in 99% D_2O (800 MHz, 50 °C).

Surprisingly, solution NMR spectra indicate a symmetric conformation of the ligand-free YRS. Clearly, any degree of structural differences between the two subunits should be reflected in the number of correlations observed in NMR spectra. It may be difficult to estimate the exact number of ^1H – ^{15}N correlations from the HSQC-TROSY⁴ map of ligand-free *Bst*-YRS (Figure 1a) because of (i) resonance overlap, (ii) missing correlations due to fast exchange with the solvent, or (iii) incomplete back-protonation of amides after protein production in D_2O . For example, only ~75% (78%) of the total number of observable amide correlations could be identified in YRS (ΔYRS) in ^1H – ^{15}N HSQC-TROSY spectra, whereas 3D HNCOTROSY data sets provided ~85% of the expected correlations for non-back-exchanged YRS and ΔYRS . It is much more straightforward to obtain the exact number of correlations in selectively methyl-labeled samples. Figure 1b–d shows that the number of methyl ^1H – ^{13}C correlations observed in the methyl-TROSY⁵ spectra of selectively [$^{13}\text{CH}_3$]-methyl-labeled full-length *Bst*-YRS closely matches the number of corresponding residues in the amino-acid sequence of the protein, indicating the lack of structural asymmetry of the ligand-free enzyme.

To ensure that the observed symmetry is not a temperature-related artifact, NMR spectra have been collected at several temperatures in the 30–50 °C range. Figure S1a in the Supporting Information shows that the changes in chemical shifts of Ala^β $^{13}\text{CH}_3$ methyls are small, indicating that no major changes in the conformations of both YRS subunits occur in this temperature range. In fact, YRS is known to form an exceptionally stable dimer ($K_D = 85 \text{ pM}$),¹⁷ it is therefore inconceivable that it dissociates under NMR conditions. At room temperature, the molecular weights of YRS and ΔYRS correspond to dimeric species based on size-exclusion chromatography elution times and PAGE electrophoresis under native conditions, whereas at higher temperatures, ^{15}N (^{13}C) relaxation times of amides (methyls) agree with those predicted for dimeric species. Likewise, temperature-dependent isothermal titration calorimetry (ITC) measurements indicate that the “half-of-the-sites” activity is retained at higher temperatures (Figure S1b; Supporting Information).

Recently, a series of NMR experiments for detection of $^{13}\text{CHD}_2$ methyl isotopomers in residually protonated large proteins produced in D_2O using [^2H , ^{13}C]-glucose as a carbon source have been developed.^{18,19} Albeit at the ~6-fold expense in sensitivity, correlations of *all* protein methyls can be detected in

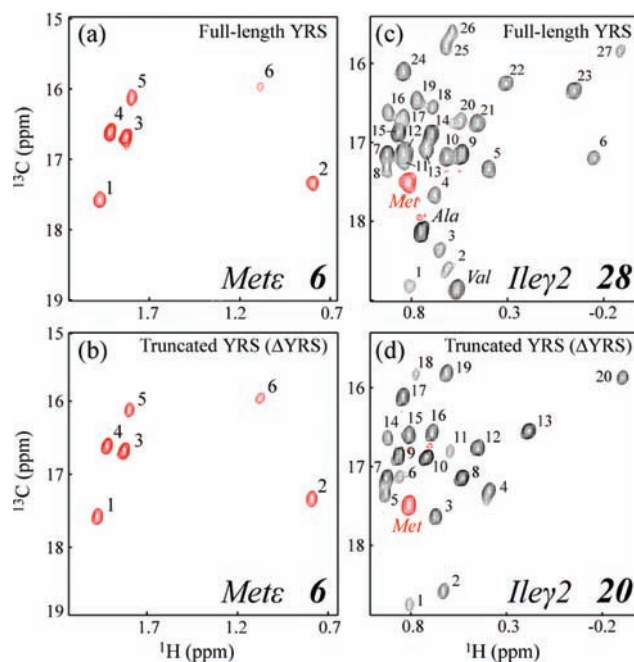


Figure 2. Selected regions of the ^1H – ^{13}C constant-time HSQC spectra showing [$^{13}\text{CHD}_2$]-methyl correlations of (a) Met^ϵ in full-length YRS; (b) Met^ϵ in ΔYRS ; (c) $\text{Ile}^{\gamma 2}$ in full-length YRS; and (d) $\text{Ile}^{\gamma 2}$ in ΔYRS . The number of residues of each type in the amino-acid sequence of YRS is shown in bold italics at the right bottom corner. Negative contours (Met) are shown in red. Met residues are absent from the C-terminal domain of YRS. All NMR data were collected at 40 °C in 99% D_2O (600 MHz).

these experiments, with Ala^β and $\text{Thr}^{\gamma 2}$ positions targeted for selective observation.¹⁸ We have applied this methodology to [^2H , ^{13}C]-labeled ΔYRS and YRS with the same result: no evidence of differences between subunit conformations on the chemical shift time-scale. Met^ϵ and $\text{Ile}^{\gamma 2}$ regions of methyl correlation maps of full-length YRS and ΔYRS are shown in Figure 2 (those not labeled with $^{13}\text{CH}_3$ methyls in Figure 1). The number of observed [$^{13}\text{CHD}_2$]-methyl correlations closely corresponds to the number of Met and Ile residues in each subunit of the homodimers. Figure S2 (Supporting Information) shows the remaining $^{13}\text{CHD}_2$ methyl correlations observed in ΔYRS ,

lending even more confidence in the absence of asymmetry of the YRS structure in solution. Note that it is especially straightforward to confirm the identification of Met methyls, as Met^ε carbons are not ¹³C-coupled to adjacent carbon positions in ¹H–¹³C HSQC correlation maps.

The homodimeric “half-site-reactive” enzyme tryptophanyl-tRNA synthetase (*Bst*-WRS; dimer MW = 74 kDa) is structurally homologous to YRS and catalyzes similar reactions of Trp activation and tRNA charging.²⁰ Several crystal structures of *Bst*-WRS free and in complexes with Trp/ATP and Trp-AMP have been solved.^{20–23} WRS crystal structures provide substantial insight into domain rearrangements during the catalytic cycle. On the basis of ATP/Trp-dependent kinetics, SAXS measurements, and X-ray structures, a mechanistic model for WRS was proposed in which ATP acts as an allosteric effector.²² The 2.9 Å crystal structure of ligand-free *Bst*-WRS (PDB ID 1D2R) shows asymmetry, although the two subunits are found in several different crystal packing environments, and the interface between the two subunits is symmetrical.²¹ We have used NMR techniques to assess the asymmetry of the unliganded homodimer in solution. Figure S3 (Supporting Information) shows the ¹H–¹⁵N correlation map and selected regions of [¹³CHD₂]-methyl HSQC spectra recorded on ligand-free [U–¹⁵N, ¹³C, ²H]-*Bst*-WRS. As with YRS above, the number of amide correlations identifiable in Figure S3a (Supporting Information) falls short of the total expected from the amino-acid sequence by ~20%, whereas the number of observed methyl peaks closely corresponds to the number of methyl-bearing side-chains of each type, indicating that under the conditions used for NMR measurements, the two subunits of the WRS homodimer adopt the same conformation.

Irrespective of the degree of crystallographically observed asymmetry in aminoacyl tRNA synthetases, the intersubunit interfaces are symmetric in all available X-ray structures of ligand-free and ligated YRS, ΔYRS, and WRS. The recently solved 2.0 Å crystal structure of the ligand-free homodimeric cAMP receptor protein, CRP (also known as catabolite gene activator protein, CAP; dimer MW = 50 kDa) from *Mycobacterium tuberculosis* features an inner asymmetry that encompasses the interface between the two subunits and extends far beyond,²⁴ with the r.m.s.d. between C^α atoms of the two subunits of 3.5 Å. Figure 3a shows the ribbon diagram of *Mtb*-CRP crystal structure. Upon binding of the effector cAMP to the N-terminal domain, the protein undergoes a conformational transition that enables specific binding of DNA to the C-terminal domain and transcription initiation.^{24,25} Thus, the functional role of the crystallographically observed asymmetry in apo-*Mtb*-CRP might be the blockage of transcription in the absence of the ligand (cAMP), even though both NMR²⁶ and crystal²⁷ structures of its homologue from *Escherichia coli*, *Ec*-CRP, are symmetric homodimers (PDB IDs 2WC2, 3HIF). Interestingly, the crystal structure of the *Ec*-CRP–cAMP₂ complex²⁸ also features an asymmetric dimer, although NMR studies clearly show that there is a 2-fold symmetry in solution.²⁹

Using the same methodology for detection of ¹³CHD₂ methyls as above, we have conducted a brief solution study of apo-*Mtb*-CRP. Figure 3b–d shows selected regions of ¹³CHD₂ methyl correlation maps recorded on [U–¹⁵N, ¹³C, ²H]-labeled CRP (37 °C). Although in this case, the number of methyl correlations is in some instances lower than expected from the protein amino-acid content, presumably because of conformational exchange broadening, no signs of asymmetry (that could be expected to lead to “doubling” of NMR peaks) can be

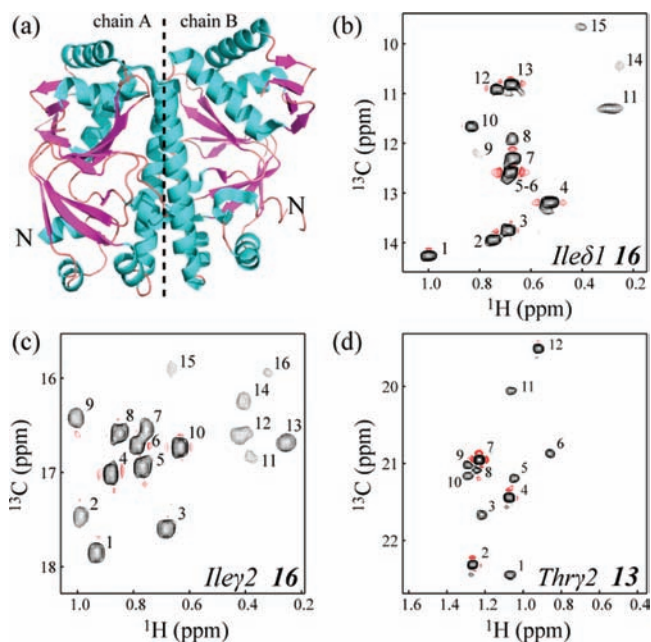


Figure 3. (a) A ribbon diagram of the crystal structure of the apo-*Mtb*-CRP homodimer (PDB ID 3D0S).²⁴ The axis of the molecular dyad is shown with a dashed vertical line. (b–d) Selected regions of the ¹H–¹³C correlation map of CRP showing [¹³CHD₂]-methyl correlations: (b) Ile^{δ1}, (c) Ile^{γ2}, (d) Thr^{γ2}. The number of residues of each type in the amino-acid sequence of *Mtb*-CRP is shown in bold italics at the right bottom corner in (b–d). Selective detection of Thr^{γ2} correlations with suppression of the rest of methyl signals has been employed.¹⁸ All NMR spectra were recorded at 37 °C in 99% D₂O (600 MHz).

observed in the spectra. We note that the dimer interface of CRP is rich in methyl-containing side-chains, especially those of Thr and Ala residues. Figure S4 of the Supporting Information shows additional regions of the ¹³CHD₂ methyl correlation map collected on [U–¹⁵N, ¹³C, ²H]-labeled apo-*Mtb*-CRP.

In view of the presented data, it is likely that the two subunits in a homodimeric protein can sample a set of different conformational substates. Some of these substates are apparently preferred in crystals, whereas they may be averaged in solution leading to the observation of a single set of NMR resonances. In half-site-reactive aminoacyl-tRNA synthetases, functional asymmetry does not appear to require pre-existent structural differences between the two subunits. The half-of-the-sites activity in YRS might result from the equilibrium between various conformational substates of the two subunits in solution.^{29,30} For example, the interconversion between catalytically active/inactive and inactive/active subunit conformations of the homodimer may occur fast on the chemical shift time-scale; i.e., asymmetric conformational states are populated only transiently, resulting in a single set of peaks in NMR spectra.³⁰ Crystal growth might selectively enforce crystallization of such states. This possibility can be addressed by NMR relaxation approaches including relaxation dispersion measurements. At this point, however, NMR relaxation measurements that sample protein dynamics on the fast (ps-to-ns) or slow (μs-to-ms) time-scales performed on *Bst*-YRS/ΔYRS and *Mtb*-CRP did not provide unequivocal experimental confirmation of this hypothesis.

Such a “dynamics-driven” asymmetry in homodimers may be captured upon initial binding of a substrate to one of the subunits, thus committing the dimer to an asymmetric state in

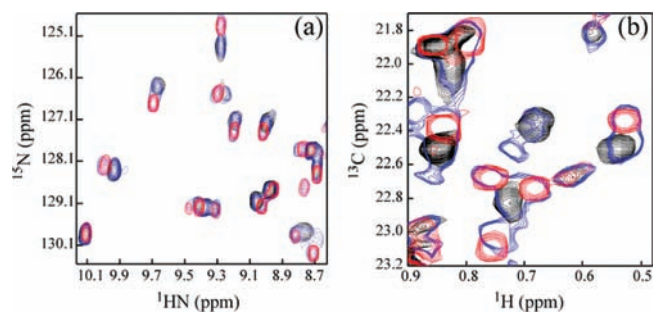


Figure 4. Selected regions of (a) ^1H - ^{15}N HSQC-TROSY and (b) methyl ^1H - ^{13}C HMQC correlation map of $[\text{U}\{-^2\text{H}, ^{15}\text{N}\}; \text{L}, \text{V}\{-^{13}\text{CH}_3/^{12}\text{CD}_3\}]$ -*Mtb*-CRP showing the changes accompanying addition of cAMP. Black contours correspond to the ligand-free *Mtb*-CRP. Red contours show *Mtb*-CRP saturated with cAMP, whereas blue peaks correspond to an intermediate concentration of cAMP so that only one of the subunits is bound predominantly.

which the second subunit is rendered inactive. YRS, for example, is expected to become distinctly asymmetric when it is half-occupied. Figure S5 (Supporting Information) shows a superposition of a region of methyl-TROSY maps recorded on full-length *Bst*-YRS in the ligand-free form and in complex with the intermediate Tyr-AMP. The concentration of Tyr (and hence Tyr-AMP) is adjusted so that only one subunit of the YRS dimer forms the complex, whereas the other subunit remains ligand-free. Three types of changes in peak positions³⁰ can be noted: (i) chemical shift does not change between the free and ligated states in both subunits (e.g., belonging to the C-terminal domain that does not interact with Tyr-AMP); (ii) “doubling” of peaks (conformational changes are confined to the ligated subunit), and (iii) peaks of both subunits change positions (corresponding to conformational changes in both subunits upon complex formation). The observed pattern of changes in peak positions is consistent with the predicted disruption of symmetry.

In the case of *Mtb*-CRP, the binding of the allosteric effector cAMP is noncooperative and occurs independently to both subunits.²⁵ The pattern of changes in peak positions in *Mtb*-CRP as a function of cAMP concentration is illustrated in Figure 4. The addition of saturating amounts of cAMP apparently leads to the symmetric *Mtb*-CRP-cAMP₂ complex.

■ ASSOCIATED CONTENT

Supporting Information. Figure S1 showing $^{13}\text{CH}_3$ -Ala $^\beta$ methyl correlation maps and ITC measurements acquired on *Bst*-YRS as a function of temperature. Figure S2 showing selected regions of the $^{13}\text{CHD}_2$ methyl correlation map of *Bst*- Δ YRS. Figure S3 showing ^1H - ^{15}N HSQC-TROSY and selected regions of the $^{13}\text{CHD}_2$ methyl spectrum of *Bst*-WRS. Figure S4 showing selected regions of the $^{13}\text{CHD}_2$ methyl correlation map of *Mtb*-CRP. Figure S5 showing the superposition of NMR spectra of the apo-YRS and the half-stoichiometric YRS-Tyr-AMP complex. This material is available free of charge via the Internet at <http://pubs.acs.org>.

■ AUTHOR INFORMATION

Corresponding Author
vitali@umd.edu

■ ACKNOWLEDGMENT

The authors thank Profs. Paul Paukstelis and Dorothy Beckett (University of Maryland) for the gift of the plasmid encoding *Bst*-YRS and access to ITC instrumentation, respectively, Dr. Prasad Reddy (NIST) for providing the plasmid of *Mtb*-CRP, and Prof. Eric First (LSU Health Center) for stimulating discussions.

■ REFERENCES

- (1) Brown, J. H. *Protein Sci.* **2006**, *15*, 1.
- (2) Creighton, T. E. *Proteins: Structures and Molecular Properties*; Freeman & Co.: New York, 1993.
- (3) Nagradova, N. K. *FEBS Lett.* **2001**, *487*, 327.
- (4) Pervushin, K.; Riek, R.; Wider, G.; Wüthrich, K. *Proc. Natl. Acad. Sci. U. S. A.* **1997**, *94*, 12366.
- (5) Tugarinov, V.; Hwang, P. M.; Ollershaw, J. E.; Kay, L. E. *J. Am. Chem. Soc.* **2003**, *125*, 10420.
- (6) Ruschak, A. M.; Kay, L. E. *J. Biomol. NMR* **2010**, *46*, 75.
- (7) Fersht, A. *Structure and Mechanism in Protein Science*, 2nd ed.; Freeman & Co.: New York, 2002.
- (8) Fersht, A. R. *Biochemistry* **1987**, *26*, 8031.
- (9) Ward, W. H.; Fersht, A. R. *Biochemistry* **1988**, *27*, 5525.
- (10) Ward, W. H.; Fersht, A. R. *Biochemistry* **1988**, *27*, 1041.
- (11) Waye, M. M.; Winter, G.; Wilkinson, A. J.; Fersht, A. R. *EMBO J.* **1983**, *2*, 1827.
- (12) Brick, P.; Bhat, T. N.; Blow, D. M. *J. Mol. Biol.* **1989**, *208*, 83.
- (13) Guijarro, J. I.; Pintar, A.; Prochnicka-Chalufour, A.; Guez, V.; Gilquin, B.; Bedouelle, H.; Delepierre, M. *Structure* **2002**, *10*, 311.
- (14) Brick, P.; Blow, D. M. *J. Mol. Biol.* **1987**, *194*, 287.
- (15) Fersht, A. R. *Biochemistry* **1975**, *14*, 5.
- (16) Ward, W. H.; Fersht, A. R. *Biochemistry* **1988**, *27*, 5525.
- (17) Park, Y. C.; Bedouelle, H. *J. Biol. Chem.* **1998**, *273*, 18052.
- (18) Guo, C.; Tugarinov, V. *J. Biomol. NMR* **2010**, *46*, 127.
- (19) Otten, R.; Chu, B.; Krewulak, K. D.; Vogel, H. J.; Mulder, F. A. J. *Am. Chem. Soc.* **2010**, *132*, 2952.
- (20) Doublet, S.; Bricogne, G.; Gilmore, C.; Carter, C. W., Jr. *Structure* **1995**, *3*, 17.
- (21) Ilyin, V. A.; Temple, B.; Hu, M.; Li, G.; Yin, Y.; Vachette, P.; Carter, C. W., Jr. *Protein Sci.* **2000**, *9*, 218.
- (22) Retailleau, P.; Huang, X.; Yin, Y.; Hu, M.; Weinreb, V.; Vachette, P.; Vonrhein, C.; Bricogne, G.; Roversi, P.; Ilyin, V.; Carter, C. W., Jr. *J. Mol. Biol.* **2003**, *325*, 39.
- (23) Retailleau, P.; Weinreb, V.; Hu, M.; Carter, C. W., Jr. *J. Mol. Biol.* **2007**, *369*, 108.
- (24) Gallagher, D. T.; Smith, N.; Kim, S. K.; Robinson, H.; Reddy, P. T. *J. Biol. Chem.* **2009**, *284*, 8228.
- (25) Stapleton, M.; Haq, I.; Hunt, D. M.; Arnvig, K. B.; Artymiuk, P. J.; Buxton, R. S.; Green, J. J. *J. Biol. Chem.* **2010**, *285*, 7016.
- (26) Popovych, N.; Tzeng, S. R.; Tonelli, M.; Ebright, R. H.; Kalodimos, C. G. *Proc. Natl. Acad. Sci. U. S. A.* **2009**, *106*, 6927.
- (27) Sharma, H.; Yu, S.; Kong, J.; Wang, J.; Steitz, T. A. *Proc. Natl. Acad. Sci. U. S. A.* **2009**, *106*, 16604.
- (28) Passner, J. M.; Schultz, S. C.; Steitz, T. A. *J. Mol. Biol.* **2000**, *304*, 847.
- (29) Tzeng, S. R.; Kalodimos, C. G. *Nature* **2009**, *462*, 368.
- (30) Popovych, N.; Sun, S.; Ebright, R. H.; Kalodimos, C. G. *Nat. Struct. Mol. Biol.* **2006**, *13*, 831.